Device

Article

# Bioelectronic drug-free control of opportunistic pathogens through selective excitability

## Graphical abstract

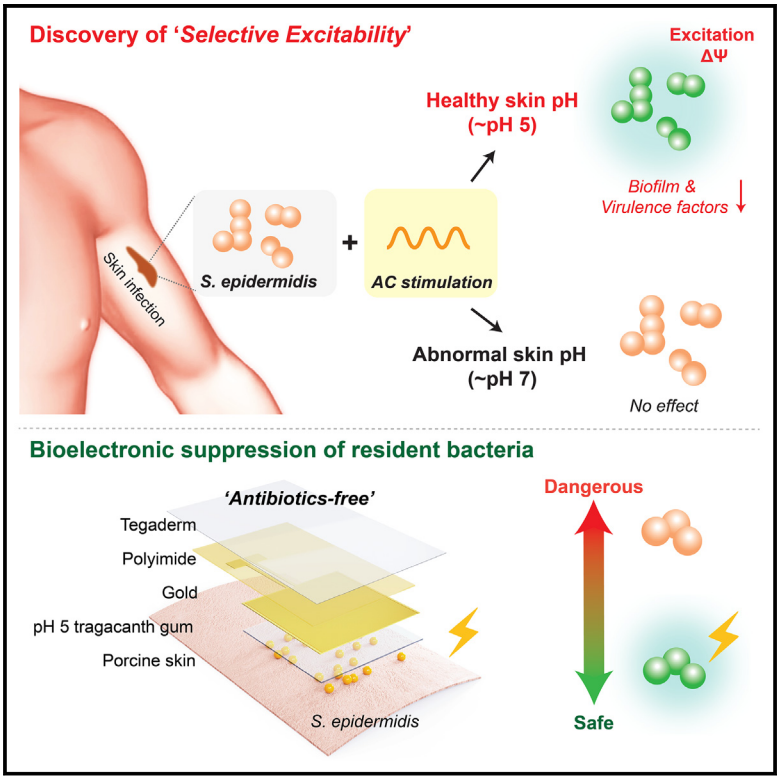


## Highlights

- Healthy skin pH confers electrical excitability to *Staphylococcus epidermidis*
- The electrically sensitized bacteria are suppressed by mild electrical stimulation
- Flexible bioelectronic device reduces bacterial biofilms on porcine skin

## Authors

Saehyun Kim, Ethan Eig, Jiping Yue, ..., Vanessa Tian, Gürol M. Süel, Bozhi Tian

## Correspondence

gsuel@ucsd.edu (G.M.S.), btian@uchicago.edu (B.T.)

## In brief

*Staphylococcus epidermidis* is a skin-dwelling bacterium responsible for common clinical infections. In this study, we discovered that *S. epidermidis* becomes electrically excitable when exposed to the acidic pH of healthy skin. This excitability enables antibiotics-free, bioelectronic suppression of the opportunistic pathogen using mild stimulation conditions.

1 Understand
Early stage research on device properties, design, and physics

Kim et al., 2024, Device 2, 100596
November 15, 2024 
Published by Elsevier Inc.
https://doi.org/10.1016/j.device.2024.100596

CellPress

Device

CellPress
OPEN ACCESS

Article

# Bioelectronic drug-free control of opportunistic pathogens through selective excitability

Saehyun Kim,[1] Ethan Eig,[1] Jiping Yue,[1] Albert Yang,[2] Colin J. Comerci,[2] Megan Laune,[1] Chuanwang Yang,[3] Ananth Kamath,[3] Jiuyun Shi,[4] Pengju Li,[5] Zhe Cheng,[1] Changxu Sun,[5] Tiantian Guo,[3] Vanessa Tian,[1] Gürol M. Süel,[2,6,7,*] and Bozhi Tian[1,3,8,9,*]

[1]Department of Chemistry, University of Chicago, Chicago, IL 60637, USA
[2]Molecular Biology Section, Division of Biological Sciences, University of California, San Diego, La Jolla, CA 92093, USA
[3]The James Franck Institute, University of Chicago, Chicago, IL 60637, USA
[4]Department of Chemical Engineering, Stanford University, Stanford, CA 94305, USA
[5]Pritzker School of Molecular Engineering, University of Chicago, Chicago, IL 60637, USA
[6]UCSD Synthetic Biology Institute, University of California, San Diego, La Jolla, CA 92093, USA
[7]Center for Microbiome Innovation, University of California, San Diego, La Jolla, CA 92093, USA
[8]The Institute for Biophysical Dynamics, University of Chicago, Chicago, IL 60637, USA
[9]Lead contact
*Correspondence: gsuel@ucsd.edu (G.M.S.), btian@uchicago.edu (B.T.)
https://doi.org/10.1016/j.device.2024.100596

**THE BIGGER PICTURE** Mammalian cells, like neurons and cardiomyocytes, are electrically excitable. Devices such as pacemakers and neural stimulators exploit this trait for drug-free electrical therapies. In contrast, the excitability of resident bacteria has been less explored, despite their crucial role in human health. If the excitability of human microbiota could be similarly harnessed for drug-free bioelectronic control, it could provide solutions to antibiotic resistance in opportunistic infections.

In this study, we explored the electrical excitability of *Staphylococcus epidermidis*, a skin-dwelling bacterium responsible for common clinical infections. While unresponsive at neutral pH, we found that the bacteria became electrically excitable in the acidic environment of healthy skin. We termed this "selective excitability," as the bacteria were selective or picky about the environment in which they displayed excitability. Exploiting the selective excitability, we suppressed bacterial virulence factors with mild electrical stimulation. This method offers localized, programmable, and antibiotic-free methods to control opportunistic pathogens.

## SUMMARY

The natural excitability in mammalian tissues has been extensively exploited for drug-free electroceutical therapies. However, it is unclear whether bacterial residents on the human body are equally excitable and whether their excitability can also be leveraged for drug-free bioelectronic treatment. Using a microelectronic platform, we examined the electrical excitability of *Staphylococcus epidermidis*, a skin-residing bacterium responsible for widespread clinical infections. We discovered that a non-lethal electrical stimulus could excite *S. epidermidis*, inducing reversible changes in membrane potential. Intriguingly, *S. epidermidis* became excitable only under acidic skin pH, indicating that the bacteria were "selective" about the environment in which they display excitability. This selective excitability enabled programmable suppression of biofilm formation using benign stimulation voltages. Lastly, we demonstrated the suppression of *S. epidermidis* on a porcine skin model using a flexible electroceutical patch. Our work shows that the innate excitability of resident bacteria can be selectively activated for drug-free bioelectronic control.

## INTRODUCTION

Leveraging the innate electrical excitability of eukaryotic cells has enabled bioelectrical modes of tissue modulation, providing alternatives to drug-based therapies. Excellent examples are electroceuticals, therapeutic bioelectronic devices that stimulate the body's naturally excitable circuits.[1] Bioelectronic devices such as cardiac pacemakers,[2,3] retinal prostheses,[4,5] and nerve stimulators[6] demonstrate how understanding and harnessing natural excitability in tissues can bring extensive health benefits.

In these devices, well-known excitable cells such as neurons have been the main target of modulation.[7,8] However, the recent discovery of innate electrical excitability in microbes suggests a potential for the bioelectrical control of commensal bacteria that are crucial to human health.[9] To target bacteria inhabiting the human body, it would be preferable to use low-voltage stimulation to modulate bacterial physiology and pathology similarly to how electroceuticals are used in human medicine.

There is a need to effectively control the bacteria residing on the human body, as many of them can become opportunistic pathogens under certain conditions.[10] For example, *Staphylococcus epidermidis*, commonly found on healthy skin, typically promotes tissue homeostasis and aids in wound healing.[11] However, factors such as compromised skin barrier, immunosuppression, and biofilm formation can shift its behavior toward pathogenicity.[12,13] In the virulent state, *S. epidermidis* is a significant contributor to neonatal morbidity[14] and is the second-leading cause of hospital infections due to the formation of antibiotic-resistant biofilm in clinical implants.[15] Moreover, the severity of dermatological disorders like atopic dermatitis[16] and scalp seborrheic dermatitis (i.e., dandruff)[17] is linked to an over-proliferation of *S. epidermidis* on the skin. Effective management of opportunistic pathogens is a major challenge that, if overcome, could have far-reaching implications.

Bioelectronic control of opportunistic pathogens may offer unique advantages over antibiotic treatments. Antibiotics carry widespread side effects, such as nausea, drug fever, and nephrotoxicity.[18] Repeated exposure to antibiotics increases the risk factor for chronic inflammatory disorders[19] and contributes to antimicrobial resistance, a global health threat.[20,21] Recently, three strains of *S. epidermidis* that are pan-resistant to all classes of antibiotics have emerged,[22] exposing the fragility of drug-based methods. Unlike drugs, bioelectrical treatments may allow for localized and targeted therapy, thereby minimizing systemic side effects.[23] Bioelectronic methods may also be applied automatically with programmable stimulation parameters that can be optimized for individual patients to enable personalized medication.[24,25]

Despite being a potential drug-free alternative, existing electrical treatment for bacteria is less developed compared to those acting on mammalian systems, as bacterial electrophysiology is still being elucidated. Conventional electrical treatment for bacteria has primarily focused on the electrostatic surface detachment of cells, high-voltage electroporation, and electrochemical biocide generation that irreversibly kills bacteria.[26–28] This contrasts with electroceuticals targeting mammalian tissues that leverage innate cellular excitability to elicit non-lethal and programmable bioelectrical responses.[29] Given that bioelectrical potential is closely related to growth, virulence, and antibiotic resistance in bacteria,[30] bioelectronic devices that exploit excitatory responses in opportunistic pathogens could offer a powerful handle to steer bacterial physiology in our favor (Figure 1A).

Several gaps in knowledge must be filled to engineer devices that can exploit excitatory responses in opportunistic pathogens. Among the human microbiota, only two species have been conclusively shown to be electrically excitable, demonstrating the ability to generate changes in membrane potential in response to electrical stimulation.[31] Specifically, *Escherichia coli* and *Bacillus subtilis*, which reside in the gastrointestinal tract, exhibit changes in membrane potential when electrically stimulated.[32] This number of reported electrically excitable species is remarkably small compared to the thousands of bacterial species that reside in our bodies.[33] Consequently, molecular mechanisms underlying bacterial electrophysiology have only been elucidated for a few model organisms such as *B. subtilis*,[9,34,35] and far less is known about more medically relevant species. Furthermore, the long-term effects and the clinical relevance of excitatory responses in opportunistic pathogens remain unclear.[31,36] This gap in understanding has impeded the development of wearable or implantable bioelectronics designed to control resident bacteria by harnessing their innate electrical excitability.

In this study, we engineered a microelectronic platform to examine the electrical excitability of the skin-residing opportunistic pathogen *S. epidermidis*. Our findings show that *S. epidermidis* can be excited by a non-lethal electrical stimulus, causing reversible changes in membrane potential. Intriguingly, *S. epidermidis* and other skin pathogens were excitable only when subjected to an acidic epidermal pH. Hence, we have coined the term "selective excitability" to describe excitatory behavior that occurs only under select conditions, such as in this case, the epidermal pH. The bioelectrical stimulation inhibited growth, virulence gene expression, and biofilm formation in *S. epidermidis*. Leveraging these findings, we developed an electroceutical patch that exploits selective excitability of *S. epidermidis*, preventing skin colonization using a voltage that is safe and imperceptible to humans. Our research highlights the discovery and utilization of selective excitability in bacteria, enabling drug-free bioelectronic control of opportunistic pathogens.

## RESULTS

### A tailored device platform enables the assessment of bacterial excitability in response to electrical stimulation

To observe the effects of electrical stimulation at single-cell resolution, we developed a customized setup for bacterial electrophysiology (Figure S1). Interdigitated gold electrodes were fabricated on a 0.17-mm glass coverslip, compatible with the use of 63× and 100× microscope objectives that have a short working distance (Figures 1B and 1C). Interdigitated designs enable electric potential localization between adjacent fingers for effective cell modulation (Figure S2),[37,38] while gold provides superior biocompatibility.[39] After inoculating the bacteria on agarose pads, these were placed on the electrode surface, and a potentiostat was used to deliver an alternating current (AC) at specified frequencies and voltages. The electrodes were designed with a width and gap of 40 μm (Figure 1D), suitable for the small size of *S. epidermidis*, which ranges from approximately 1 to 2 μm.[40] Incorporating a 2 × 2 grid within a single device enabled us to perform parallel experiments with varying conditions, facilitating statistical analysis. The customized setup allowed us to deliver exogenous electrical stimuli and monitor

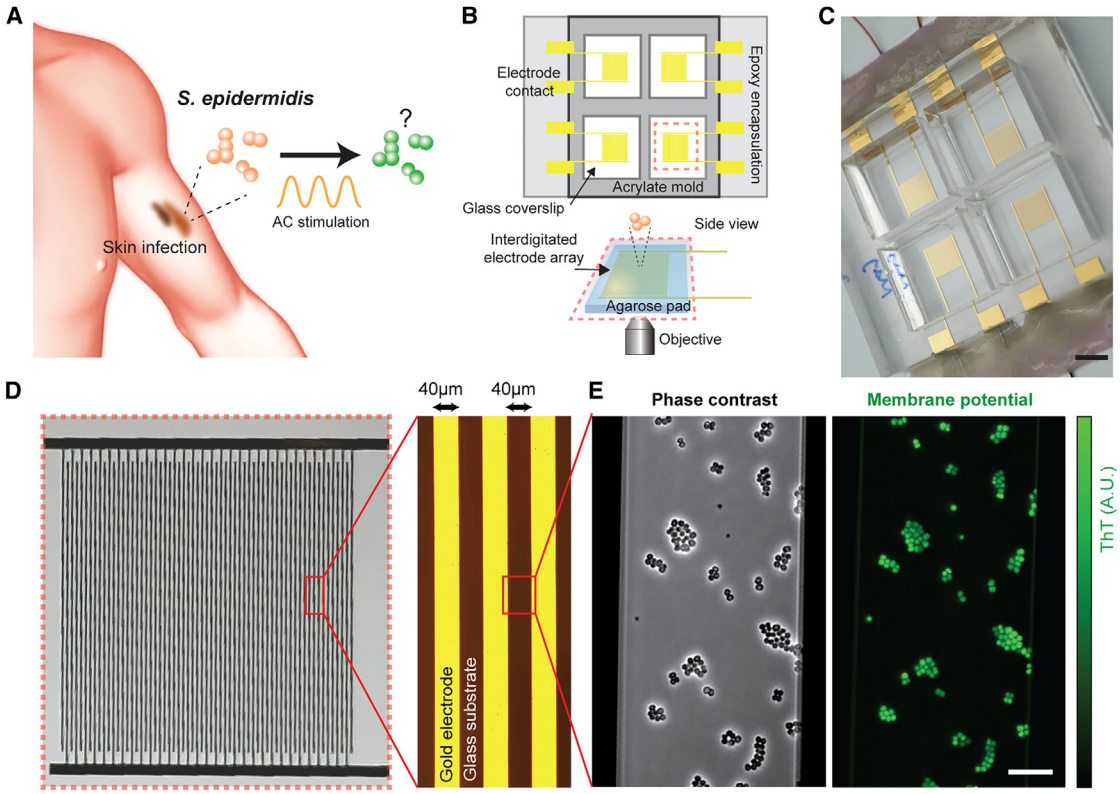


**Figure 1. An interdigitated stimulation platform enables the assessment of bacterial excitability in response to electrical stimulation**

(A) Opportunistic infections by *S. epidermidis* serve as a leading source of healthcare-associated infections. We investigate whether we can induce an excitatory response in *S. epidermidis* through electrical stimulation, enabling drug-free, bioelectrical modulation.

(B) Schematics of the electrical simulation device used to study the excitability of *S. epidermidis*.

(C) The electrical stimulation device. Scale bar, 5 mm.

(D) Magnified image of interdigitated gold microelectrodes.

(E) Phase contrast (left) and fluorescence image of ThT-stained *S. epidermidis* (right) located between the interdigitated gold electrode array. ThT reports on the membrane potential. The color bar illustrates the intensity range of ThT-stained cells. Scale bar, 10 μm.

electrophysiological changes in bacteria through fluorescence and phase-contrast microscopy (Figure 1E).

## Epidermal pH confers electrical excitability to *S. epidermidis*

Skin-residing bacteria are exposed to diverse pH conditions, with healthy skin typically ranging from 4.7 to 5.2[41] and skin with atopic dermatitis from 5.5 to 5.9.[42] Acne vulgaris presents a skin pH of around 6.4,[43] whereas chronic wounds have pH varying from 7.2 to 8.9.[44] Considering the varied environmental pH levels to which the bacteria are subjected, we explored the electrical excitability of *S. epidermidis* across external pH ($pH_e$) ranges of 4–9. The electrical stimulation condition (75 millivolts peak-to- peak [mVpp]/μm, AC, 0.1 kHz for 10 s) was selected based on the work on *B. subtilis* stimulation by Stratford et al.[32] and optimization processes outlined in Figure S3.

Electrical stimulation increased the fluorescence intensity of the membrane potential indicator thioflavin T (ThT) in cells, indicative of hyperpolarization (Video S1). However, this response was observed only at $pH_e = 5$, matching the pH of healthy skin (Figures 2A–2C).[45] Hyperpolarization of *S. epidermidis* upon electrical stimulation was confirmed with another membrane potential indicator, tetramethylrhodamine (Figure S4). We also studied changes in the bacteria's intracellular pH using pHrodo staining. Electrical stimulation increased pHrodo fluorescence, suggesting cytoplasmic acidification. Like the membrane potential, the change was observed only at $pH_e = 5$ (Figures 2D–2F). Single-cell traces of ThT and pHrodo fluorescence showed that the excitatory response occurs across the population (Figure S5).

An acidic epidermal pH, used as the skin's first line of defense against microbes, presents an adverse environment for bacterial growth.[46] Surprisingly, *S. epidermidis* exhibited electrical excitability at the epidermal pH of 5, but remained completely unresponsive to stimulation at its optimal growth condition at pH 7.4 (Figure S6). We coined the term "Selective excitability" to describe how the bacteria became excitable only when select conditions, deviating from the best thriving environment, were met.

Next, several control experiments were conducted to demonstrate the reversibility and non-lethality of the excitation response. Changes in membrane potential and intracellular pH were not due

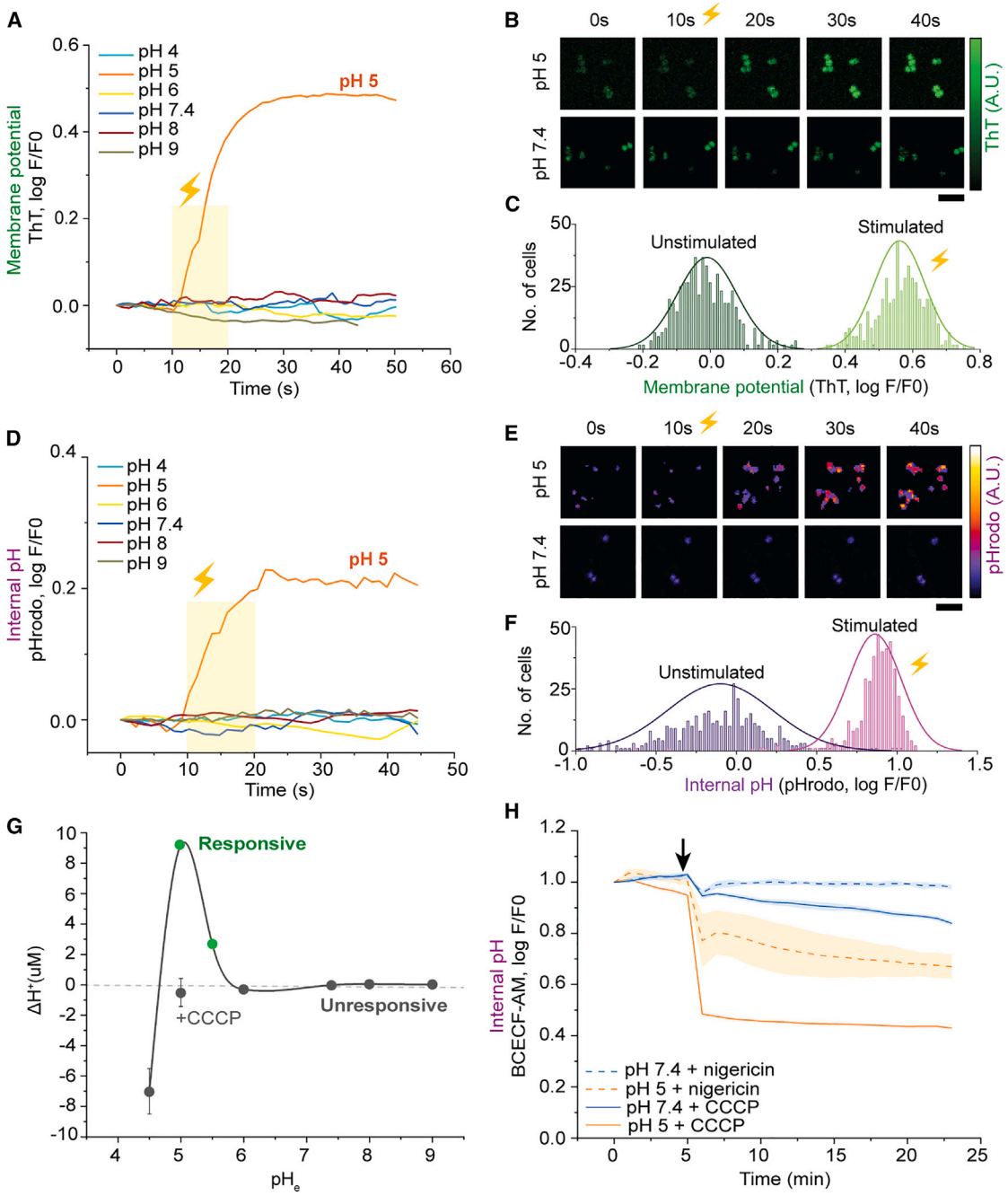


**Figure 2. Epidermal pH confers electrical excitability to *S. epidermidis***

(A) ThT intensity traces show that electrical stimulation hyperpolarizes *S. epidermidis* only at $pH_e = 5$. Fluorescence intensity is calculated as log(F/F0), where F is the fluorescence and F0 is the fluorescence at the resting state. See also Figure S2 for single cell traces.

(B) Confocal images show that electrical stimulation elicits hyperpolarization at $pH_e = 5$, but not at $pH_e = 7.4$. The pH of 7.4 represents the unmodified pH of TSB medium, where the bacteria grow most optimally. Scale bar, 5 μm. The color bar illustrates the intensity range of ThT-stained cells.

(C) Intensity histogram of ThT-stained cells at rest and post-stimulation at $pH_e = 5$ ($n \geq 300$).

(D) pHrodo intensity traces show that electrical stimulation acidifies the cytoplasm of *S. epidermidis* only at $pH_e = 5$. pHrodo reports on the internal pH, with its fluorescence increasing at a lower internal pH. See also Figure S2 for single cell traces.

(E) Confocal images show that electrical stimulation induces acidification of cytoplasm at $pH_e = 5$, but not at $pH_e = 7.4$. Scale bar, 5 μm. The color bar illustrates the intensity range of pHrodo-stained cells.

(F) Intensity histogram of pHrodo-stained cells at rest and post-stimulation at $pH_e = 5$ ($n \geq 300$).

*(legend continued on next page)*

to cell death or electroporation (Figure S7), as the proportion of propidium iodide-stained cells remained unchanged upon stimulation. Indeed, the electric field we applied (75 mVpp/μm) was about two orders of magnitude lower than the lethal electroporation threshold for *S. epidermidis* reported in the literature, which ranges from 1,000–3,500 mV/μm.[47] The electric field was generated with an AC voltage ($V_{ac}$) of 1.5 $V_{ac}$, which is considered safe and imperceptible to humans.[48] Importantly, the hyperpolarized membrane potential could be reversed back to the resting state within a 6-h time frame, during which the bacteria resumed growth (Figure S8). These results show the reversibility and non-lethal nature of the bioelectrical response.

More control experiments were conducted to understand the nature of the excitatory response. Using fluorescein as a pH probe, we verified that external pH, which is known to affect membrane potential, remains unaltered during and after the stimulation (Figure S9). Furthermore, we found that the excitation laser for ThT and pHrodo alone does not trigger an increase in fluorescence (Figure S10). The simultaneous rise in ThT and pHrodo fluorescence during electrical stimulation aligned with reported connections between internal pH and membrane potential. Specifically, it is known that the decrease in internal pH is balanced by hyperpolarization of the membrane potential as part of bacterial pH homeostasis (see Figure S11 for details).[49,50] Overall, the experiments suggested that the observed phenomenon is an authentic electrophysiological response elicited by electrical stimulation.

Next, we investigated why bacteria only responded at pH 5 and how the epidermal pH confers excitability to *S. epidermidis*. By using the intracellular pH dye BCECF-AM, we found that the transmembrane proton gradient $\Delta H^+$ is small at $pH_e \geq 6$, and collapses at acidic $pH_e \leq 4.5$. The $\Delta H^+$, however, strongly peaks at $pH_e = 5$ (Figure 2G). Since electrical excitation of *S. epidermidis* involves proton influx, the large $\Delta H^+$ near epidermal pH can be correlated with a greater driving force for the electrical response. Indeed, we observed that *S. epidermidis* can be excited only when significant $\Delta H^+$ is present, at pH 5 and 5.5 (Figure S12). Conversely, abolishing the proton gradient by adding the protonophore carbonyl cyanide *m*-chlorophenyl hydrazone (CCCP) completely inhibited the excitation response (Figure S13). The results indicated that the presence of $\Delta H^+$ is critical for the excitability of *S. epidermidis*.

To demonstrate how large $\Delta H^+$ drives proton influx when cells are perturbed, we conducted kinetic measurements of BCECF-AM fluorescence (Figure 2H). Upon adding CCCP and nigericin, two ionophores known to induce proton influx, there is a significant drop in BCECF-AM fluorescence, indicative of cytoplasmic acidification, at $pH_e = 5$. At $pH_e = 7.4$, however, the change is less pronounced. The differences were expected as $\Delta H^+$ at $pH_e = 5$ is orders of magnitude larger than at $pH_e = 7.4$ (Figure 2G). The result suggests that selective excitability at the epidermal pH range of 5–5.5 arises due to a large $\Delta H^+$ gradient, which provides driving force for proton influx when perturbations, such as electrical stimulation, are applied.

Interestingly, we also noted that epidermal pH confers electrical excitability to other opportunistic pathogens—*S. capitis* and *S. saprophyticus*. *S. capitis*, part of the normal skin flora, causes opportunistic infections in prosthetic medical devices and neonatal sepsis.[51] *S. saprophyticus*, prevalent in the acidic environment of the skin, vagina, and urogenital tract, is responsible for 10%–20% of urinary tract infection in sexually active young women worldwide.[52] Upon electrical stimulation, *S. capitis* displays hyperpolarization at $pH_e = 5$ but not at $pH_e = 7.4$ (Figures 3A and 3B). Similar to *S. epidermidis*, the driving force for proton influx, $\Delta H^+$, was two orders of magnitude larger at $pH_e = 5$ than at $pH_e = 7.4$ (Figure 3C). Identical trends were observed for *S. saprophyticus* (Figures 3D–3F). The results demonstrate the existence of selective excitability in the skin-residing microbes that were previously not known to be excitable. While exploring trends in the electrical response of resident bacteria is beyond the scope of this paper, future investigation into this topic will help determine how selectively electrical stimulation can modulate bacteria on skin (Figure S14).

## Programmable electrical stimulation suppresses virulence factors in *S. epidermidis*

We next aimed to understand the long-term effects of electrical stimulation on *S. epidermidis* at a population level. We observed that electrical stimulation reduces both growth and ATP levels in *S. epidermidis* with successive stimulation cycles (Figure 4A). This was expected, since perturbations in membrane potential and intracellular pH have been reported to interfere with normal cellular functions, including proliferation and respiration.[53,54] The reduction was not observed at $pH_e = 7.4$, where no excitation response was observed. Moreover, transcriptional analysis post-electrical stimulation revealed a decrease in the expression of virulence genes responsible for surface adhesion (*SdrG*), polysaccharide intracellular adhesin (*icaB*, *icaC*), protease (*Clp*), oxidative damage resistance (*MsrA*), and virulence regulation (*SarA*) (Figure 4B).[12,55,56] The results show that the excitatory response accompanies a suppressive effect on the virulence of the opportunistic pathogen.

We further investigated whether electrical stimulation could assist in controlling biofilm formation, the defining virulence factor in *S. epidermidis*.[57] Given that electrical stimulation hyperpolarizes *S. epidermidis*, making the cells more negatively charged, we hypothesized that this would electrostatically increase the vulnerability of the cell to positively charged aminoglycoside antibiotics such as gentamicin (Figure S15). Indeed, co-staining *S. epidermidis* with ThT and gentamicin-Texas red (GTTR) shows that repeated stimulation leads to successive hyperpolarization and accumulation of gentamicin (Figure 5A). Hence, we programmed a protocol to enhance the inhibitory effect of a drug

(G) The maximum of transmembrane proton gradient, $\Delta H^+$, exists near $pH_e = 5$, which could be abolished by the addition of 150 μM CCCP ($n = 4$). Experimentally, cells are electrically excitable (green) only near the epidermal pH, where substantial $\Delta H^+$ is present.
(H) Upon addition of CCCP (150 μM) and nigericin (3 μM), *S. epidermidis* shows greater cytoplasmic acidification at $pH_e = 5$ compared to $pH_e = 7.4$. BCECF-AM reports on internal pH, with its fluorescence decreasing at a lower internal pH. The black arrow denotes the point of addition ($n = 4$).
All data are presented as means ±SDs.

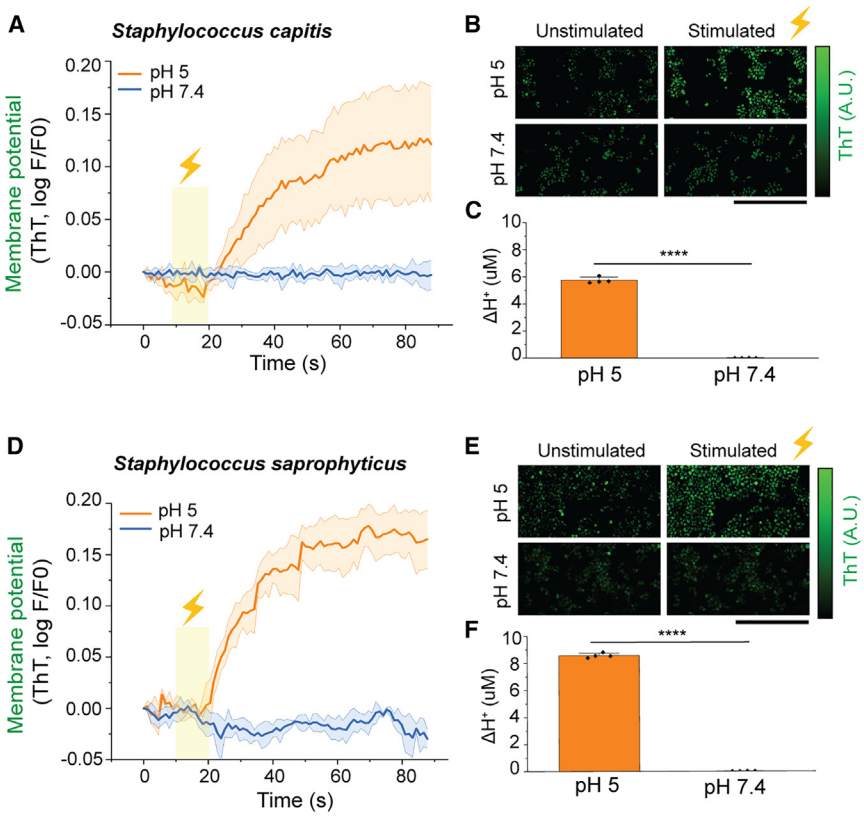


**Figure 3. Epidermal pH confers selective excitability to two other skin-residing opportunistic pathogens**

(A) Mean ThT intensity traces show that electrical stimulation hyperpolarizes *S. capitis* at $pH_e = 5$, but not at $pH_e = 7.4$ ($n = 5$).

(B) Confocal images show that electrical stimulation at $pH_e = 5$ hyperpolarizes *S. capitis*, but not at $pH_e = 7.4$. Scale bar, 20 μm. The color bar illustrates the intensity range of ThT-stained cells.

(C) The transmembrane proton gradient of *S. capitis* at $pH_e = 5$ is significantly larger than at $pH_e = 7.4$ ($n = 4$).

(D) ThT intensity traces show that electrical stimulation hyperpolarizes *S. saprophyticus* at $pH_e = 5$, but not at $pH_e = 7.4$ ($n = 5$).

(E) Confocal images show that electrical stimulation at $pH_e = 5$ hyperpolarizes *S. saprophyticus*, but not at $pH_e = 7.4$. Scale bar, 20 μm. The color bar illustrates the intensity range of ThT-stained cells.

(F) The transmembrane proton gradient of *S. saprophyticus* at $pH_e = 5$ is significantly larger than at $pH_e = 7.4$ ($n = 4$).

All data are presented as means ± SDs.

through electrical pretreatment. The protocol involved 5 cycles of stimulation pretreatment to induce hyperpolarization, followed by incubation with a sublethal dose of gentamicin for 18 h. While electrical pretreatment or a sublethal dosage of gentamicin alone failed to reduce biofilm coverage by more than 30%, their combined application resulted in a 94% decrease in biofilm coverage (Figures 5B and 5C). This demonstrates that electrical stimulation can enhance the effect of the drug, enabling biofilm inhibition with reduced dosages of antibiotics.

Next, we investigated the possibility of controlling biofilm formation solely through electrical means, without the use of drugs. As mentioned earlier, *S. epidermidis* can recover its membrane potential and resume growth upon stimulation (Figure S8). Thus, we developed a protocol that applies electrical stimulation at periodic intervals, every 10 min, to prevent recovery and achieve long-term suppression. The periodic stimulation at $pH_e = 5$ eradicated biofilm formation by 99% without the need for antibiotics (Figures 5D and 5E). The effect of inhibition was localized where the bulk interdigitated electrode arrays were present (Figure S16). No reduction in biofilm formation was observed at $pH_e = 7.4$ (Figure 5F), where excitation response was not observed, indicating that the periodic electrical stimulation itself is non-lethal for the bacteria. In the absence of an excitatory response at pH 7.4, a voltage as high as 9.5 $V_{ac}$ was required to achieve a similar, albeit less effective, level of biofilm suppression using the identical protocol (Figure S17). The low-voltage and drug-free electrical suppression of biofilm growth was uniquely enabled at the epidermal pH where *S. epidermidis* displays selective excitability.

## Bioelectronic localized antimicrobial stimulation therapy

Chronic skin inflammation and wounds are linked with elevated pH levels and colonization of virulent *S. epidermidis* that can exacerbate the conditions.[16,58–61] To address the issue, we developed an electroceutical device that can restore the acidic pH of the skin, sensitizing *S. epidermidis* to electrical stimulation and suppression. The device was used to deliver bioelectronic localized antimicrobial stimulation therapy (BLAST), which controls proliferation of the opportunistic pathogen through a drug-free bioelectrical stimulation. The stimulation parameters for BLAST were set identically to the drug-free suppression protocol in Figure 5D.

The electroceutical device featured an interdigitated electrode array on a flexible polyimide (PI) substrate (Figures 6A and 6B). pH 5-adjusted tragacanth gum served as a hydrogel interlayer between the skin and device, which provided an acidic environment that confers excitability to *S. epidermidis* (Figure S18). Tragacanth gum was selected for its biocompatibility and its natural ability to form an acidic pH upon gelation.[62] With 500 cycles of periodic stimulation lasting 5 days, the device showed no significant decline in impedance, indicating its stability (Figure S19). The stimulation condition was benign for humans; we utilized a voltage of 1.5 $V_{ac}$, which is an order of magnitude below the most conservative 15-$V_{ac}$ voltage limit deemed imperceptible and safe for wet contact.[48] When we applied the device to a surface inoculated with *S. epidermidis*, together with tragacanth gum, electrical stimulation elicited the hyperpolarization response as shown by confocal z stack imaging (Figures 6C and 6D). This confirmed that our device can stimulate *S. epidermidis*.

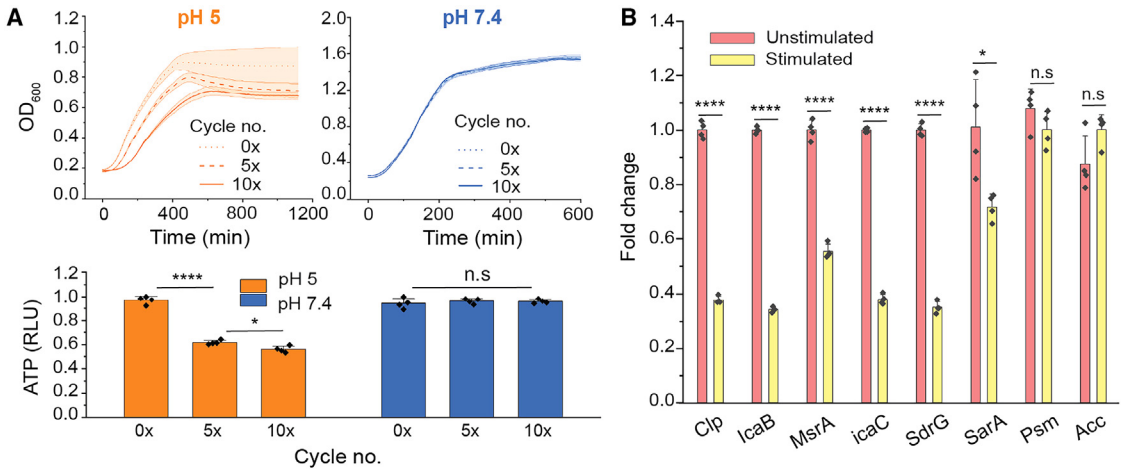


**Figure 4. Population response of *S. epidermidis* reveals the suppressive effect of electrical stimulation**

(A) Electrical stimulation reduces the growth and ATP levels in *S. epidermidis* at $pH_e$ = 5, but not at $pH_e$ = 7.4 ($n$ = 4).

(B) Electrical stimulation at $pH_e$ = 5 reduces virulence gene expression in *S. epidermidis*, measured by the RT-qPCR ($n$ = 4). The fold change was normalized relative to the expression level of the guanylate kinase (*gmk*) housekeeping gene.

Each stimulation cycle consists of a 75 mVpp/μm amplitude at 0.1 kHz AC for a duration of 10 seconds. All data are presented as means ± SDs.

To showcase the potential of BLAST in controlling opportunistic pathogens, we interfaced the device with porcine skin inoculated with *S. epidermidis*. Porcine skin was selected for its similarity to human skin.[63] After 18 h of BLAST treatment, we discovered a nearly 10-fold reduction in the colony-forming units on porcine skin for stimulated groups (Figure 6E). Scanning electron microscopy (SEM) imaging further confirmed the reduction in the porcine skin colonization by *S. epidermidis*, showing a substantial decrease in biofilm coverage (Figures 6F and 6G). Furthermore, we examined whether BLAST could be applied to control *S. epidermidis* biofilm formation on other clinically relevant surfaces. Following an identical protocol, we inoculated *S. epidermidis* on the silicone surface utilized for catheter tubing and the surface of ultra-high molecular weight polyethylene utilized for prosthetic implants. Upon applying periodic electrical stimulation, significant reduction in the colony-forming units was observed for stimulated groups (Figure S20). This demonstration highlights a bioelectronic device exploiting selective excitability of the opportunistic pathogen, enabling drug-free control.

## DISCUSSION

We engineered a microelectronic device to investigate the electrical excitability of the skin-residing opportunistic pathogen *S. epidermidis*. We discovered that *S. epidermidis* can be excited by exogenous electrical stimuli, resulting in cytoplasmic acidification and reversible changes in membrane potential. The presence of a large transmembrane proton gradient near the epidermal pH conferred selective excitability to *S. epidermidis* and other skin-residing opportunistic pathogens. The bioelectrical stimulation programmably suppressed growth and biofilm formation in *S. epidermidis*. Finally, we developed a drug-free electroceutical device that exploits the selective excitability of *S. epidermidis*, reducing its colonization on a porcine skin model through BLAST treatment.

We demonstrated that matching the acidic pH of the skin confers electrical excitability to opportunistic pathogens not previously known to be excitable. This selective excitability arises within a narrow pH range of 5–5.5, a hostile condition that deviates from the optimum growth pH for the organism. Given that bacteria have evolved mechanisms to maintain their $H^+$ gradient under varying environments, each species may possess a different regime for electrical excitation.[49,64,65] While *B. subtilis* and *E. coli* are the only two non-electroactive bacteria reported to be electrically excitable,[32,66] selective excitability could be a key to uncovering hidden excitatory responses in other microorganisms. Exploring the excitability of functional microbes may facilitate electrical control of bacterial physiology for diverse applications.[67,68]

We utilized the finding of *S. epidermidis*' selective excitability to develop a bioelectronic device for controlling bacterial physiology and pathology. Through a low-voltage AC stimulation that is safe and imperceptible to humans, we elicited a non-lethal excitation response in *S. epidermidis* through reversible changes in membrane potential. This bioelectrical method allowed us to control growth, ATP, and biofilm formation of *S. epidermidis* at a benign voltage that was ineffective to the bacteria outside their selective pH. In the absence of the excitatory response, significantly higher voltage was required to achieve a similar level of biofilm suppression while risking device degradation. Our method contrasts with conventional electrical stimulation typically used to either electrolytically kill bacteria through toxic chemicals or electroporate cells at dangerously high voltages.[26,27] Our results will promote further research into bioelectrical control of medically relevant bacteria, extending beyond lethal electroporation.

Our bioelectronic treatment not only enables drug-free control of opportunistic pathogens but also demonstrates effectiveness

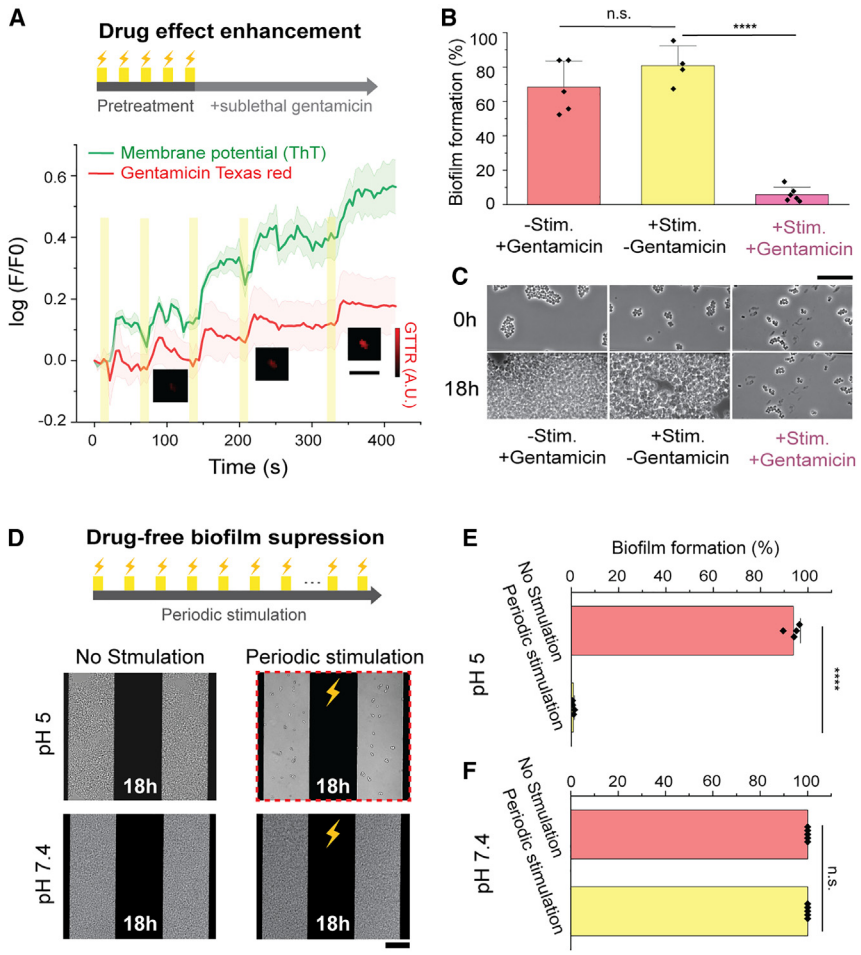


**Figure 5. Selective excitability enables programmable biofilm suppression**

(A) Mean intensity trace of *S. epidermidis* co-stained with ThT and GTTR. Electrical stimulation at $pH_e$ = 5 results in hyperpolarization accompanied by the accumulation of gentamicin ($n$ = 5). Scale bar, 5 μm. The color bar illustrates the intensity range of GTTR-stained cells.

(B) Electrical pretreatment at $pH_e$ = 5 enhances the suppressive effect of sublethal gentamicin (30 μg/mL) toward *S. epidermidis* biofilm formation ($n \geq 4$). Stim., stimulation.

(C) Phase contrast images show that electrical pretreatment at $pH_e$ = 5 combined with a sublethal gentamicin stops bacterial growth. Scale bar, 20 μm.

(D) Phase contrast images of *S. epidermidis* biofilm after 18 h of periodic electrical stimulation, applied every 10 min. Periodic stimulation abolishes biofilm formation at $pH_e$ = 5, but not at $pH_e$ = 7.4. Scale bar, 20 μm.

(E) Periodic electrical stimulation abolishes biofilm growth at $pH_e$ = 5 ($n$ = 4).

(F) Periodic electrical stimulation does not reduce biofilm growth at $pH_e$ = 7.4 ($n$ = 4), indicating a non-lethal bioelectrical stimulation condition.

Each stimulation cycle consists of a 75 mVpp/μm amplitude at 0.1 kHz AC for a duration of 10 seconds. All data are presented as means ± SDs.

and advantages over drug-based methods. Periodic electrical stimulation reduced biofilm formation by over 90%, with the reduction localized at the interdigitated electrodes. By programming the stimulation protocol, we could transition from drug-enhanced to drug-free modes of biofilm suppression. In addition, growth, ATP levels, and antibiotic accumulation could be controlled stepwise by adjusting the number of stimulation cycles. The localized, programmable, and highly controllable therapy demonstrates the unique advantages of bioelectronic treatment over antibiotics-based methods. This approach is very easy to customize for individual patients and their treatment needs.

While we demonstrated an electroceutical device that exploits the excitability of opportunistic pathogens, much more work is needed to apply the device in practical settings. Molecular-level studies are needed to identify which ion channels could be involved in mediating electrical responses in bacteria. Improved fundamental understanding of ionic responses could also enable an engineering approach to amplify the electrical response.[69,70] Also, it should be noted that AC stimulation may be less convenient for wearable device applications due to the complexity of design and higher power consumption. To improve practicality, developing power-efficient methods and optimized circuit designs is essential.[71] A better molecular understanding of bacterial stimulation mechanisms—including the role of ion channels and the contributions of capacitive and faradic components—may enable the exploration of alternative signal types for stimulation.[72]

Lastly, exploring the environmental factors that grant electrical responsivity to bacteria may offer valuable insights into the evolutionary interplay between microorganisms and their host environments. For example, the stable proton gradient at pH 5 suggests that *S. epidermidis* can endure unfavorable epidermal pH levels to maintain the driving force for ATP synthesis, surviving as a part of the commensal skin flora. From the host's perspective, evolution has maintained acidic skin pH, which is crucial for enzymatic regulation, barrier integrity, and microbial defense.[46] However, the impact of epidermal pH on conferring electrical excitability to bacterial inhabitants remains largely unexplored. The presence of natural electrical phenomena on the skin, such as *trans*-epidermal electric potential[73] and electrostatic discharge,[74] prompts intriguing questions regarding their potential influence on the electrophysiology of commensal microbes. Investigating this interaction warrants further scientific exploration.

## EXPERIMENTAL PROCEDURES

### Strains and growth conditions

*S. epidermidis* (strain NIHLM087, provided by Dr. Julia Segre at NIH, NCBI taxonomy ID: 979201) was cultured overnight in tryptic soy broth (TSB) using a shaker incubator (37°C, 200 rpm). A 1-mL sample of the overnight liquid culture (optical density 600 [$OD_{600}$] ~3.00) was pelleted and resuspended in an equal volume of pH-adjusted TSB buffer. The resuspended bacterial solution

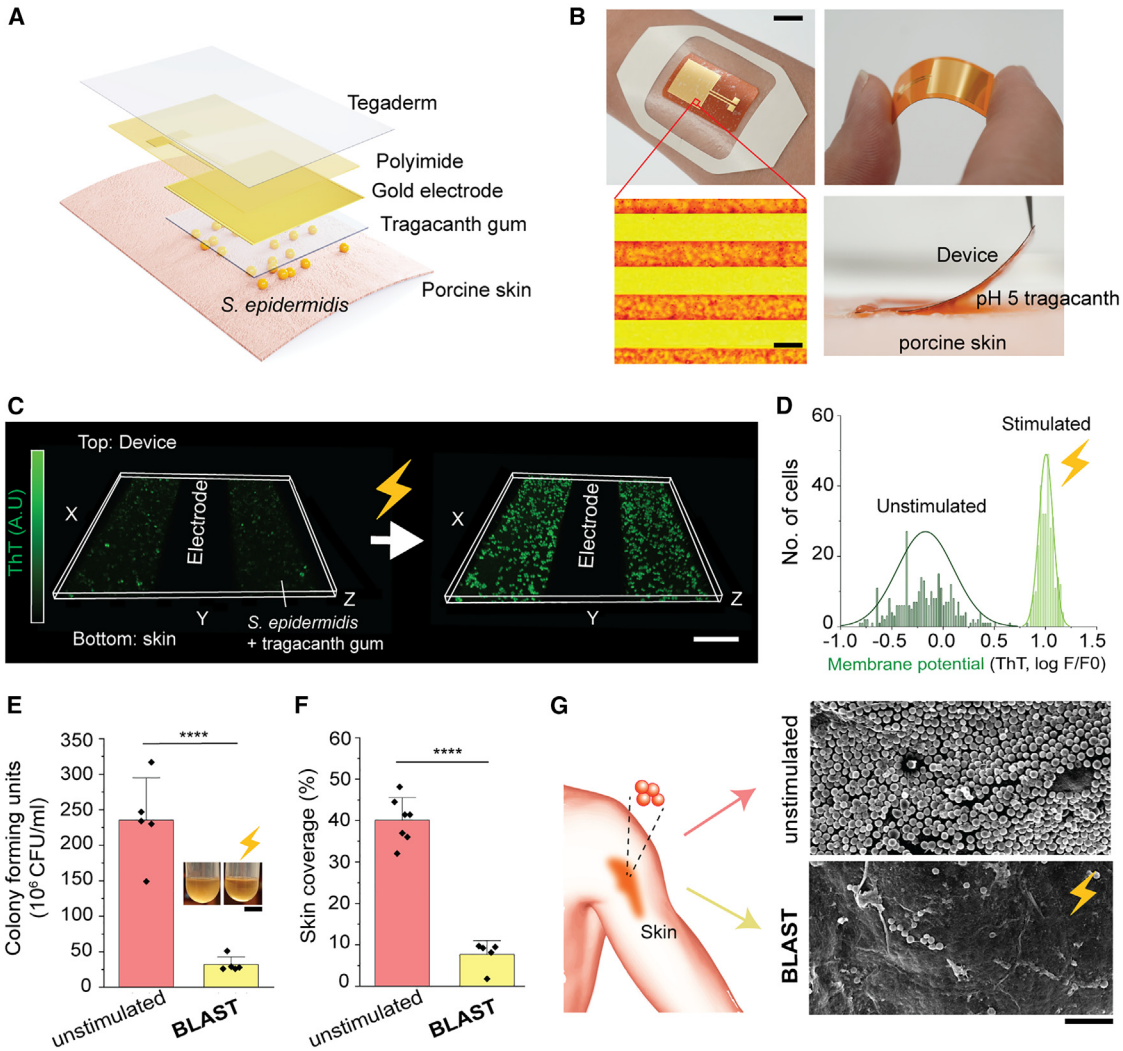


**Figure 6. BLAST reduces colonization of porcine skin by *S. epidermidis***

(A) Schematic diagram showing structural components of the electroceutical skin patch used to stimulate *S. epidermidis*.

(B) Photograph showing wearability and flexibility of the skin patch. Scale bar, 1 cm (top), 40 μm (bottom).

(C) Three-dimensional reconstruction of confocal z stack images shows hyperpolarization of ThT-stained *S. epidermidis* upon electrical stimulation. Scale bar, 20 μm. The color bar illustrates the intensity range of ThT-stained cells.

(D) ThT intensity histogram shows population-wide hyperpolarization response elicited upon electrical stimulation of *S. epidermidis* ($n \geq 600$).

(E) BLAST significantly reduces the colony-forming units of *S. epidermidis* on porcine skin after 18 h ($n = 5$). Insets show visible reduction in the opacity of *S. epidermidis* collected and cultured from porcine skin. Scale bar, 1 cm.

(F) BLAST significantly reduces the *S. epidermidis* biofilm coverage on porcine skin after 18 h ($n \geq 5$).

(G) SEM imaging shows that BLAST decreases *S. epidermidis* biofilm coverage on the porcine skin surface. Scale bar, 5 μm.

All data are presented as means ± SDs.

was then added to an aerated culture tube and incubated in the shaker incubator (37°C, 200 rpm) for 3 h.

For imaging membrane potential or antibiotics accumulation, 10 μM ThT (Acros Organics), 200 nM trimethylrhodamine (TMRM, Invitrogen), or 2 μg/mL of GTTR (AAT Bioquest) was added after 2 h of incubation. At 3 h of incubation, 1 μL cells were inoculated onto pH-adjusted TSB agarose pads containing the same concentration of ThT, TMRM, or GTTR. The inoculated agarose pad was placed on the interdigitated gold electrode device for imaging and stimulation. Imaging of bacterial viability was done using the LIVE/DEAD BacLight Bacterial Viability Kit (Molecular Probes) following the identical procedure, using suggested dye concentration from the manufacturer. The agarose pad was prepared by melting ultrapure agarose (Invitrogen), which was then solidified on a 22 × 22-mm cover glass and cut to an 8 × 8-mm size. When abolishing the transmembrane pH gradient, the agarose pad was supplemented with 150 μM of CCCP (Cayman Chemical).

For imaging of intracellular pH, 1 mL of the overnight cultured *S. epidermidis* was resuspended in 1 mL of pH 7.4 TSB. Then, 2 μL pHrodo Green AM Ester and 20 μL PowerLoad concentrate (Invitrogen) were added to the suspension and left at room temperature for 30 min. After this, the cells loaded with pHrodo were washed twice with pH 7.4 TSB and resuspended in 1 mL of the pH-adjusted TSB buffers. The bacteria were incubated for 3 h (37°C, 200 rpm) in an aerated culture tube and inoculated on a TSB agarose pad without any added dyes. The inoculated agarose pad was placed on the interdigitated gold electrode device for imaging and stimulation. An identical procedure

was used for the culturing and stimulation of *S. capitis* (American Type Culture Collection [ATCC] no. 35661), *S. saprophyticus* (ATCC no. 15305), and *E. coli* (MG1655).

### Device fabrication and characterization

To fabricate the interdigitated stimulation device for the assessment of bacterial excitability, no. 1.5 thickness microscope cover glass (Brain Research Lab, no. 4860-1.5D) was sonicated in acetone and isopropyl alcohol for 15 min. After blow drying with $N_2$, the cover glass was subjected to hexamethyldisilazane (HMDS) vapor priming. A $SiO_2$ wafer (NOVA Electronic Materials) of identical dimensions (60 × 48 mm) was spin-coated with AZ nLOF 2070 (2,500 rpm, 45 s). Following HMDS treatment, the cover glass substrate was placed on top of the photoresist-coated $SiO_2$ wafer and baked at 110°C for 3 min. This process was used to bond cover glass to the wafer substrate, reducing thermal expansion during subsequent fabrication processes. Next, the substrate was spin-coated with AZ nLOF 2020 and soft-baked at 110°C for 2 min. The substrate was exposed with a Heidelberg MLA150 Direct Write Lithographer. After a post-exposure bake at 110°C for 2 min, the pattern was developed in AZ 300 MIF for 50 s. After washing in deionized water, 10 nm titanium and 100 nm gold were deposited using an EvoVac Electron Beam Evaporator (Angstrom). The photoresist and bonding to the $SiO_2$ wafer were lifted off in Remover PG at 80°C overnight, releasing the cover glass substrate with interdigitated gold electrode patterns. Acrylic plastic (Alfa Aesar) was cut with a VLS 4.60 laser cutter to make a 2 × 2 well, which was bound to the cover glass substrate using Kwik-Sil (World Precision Instruments). The device was wired using copper wire (Remington) and PELCO conductive silver paint (Ted Pella), which was insulated with epoxy (JB Weld). For the fabrication of the electroceutical skin patch for BLAST, an identical procedure was used, replacing the cover glass substrate with PI film up to the lift-off stage using Remover PG. The released PI film with interdigitated gold electrodes was wired and attached to Tegaderm (3M). The dimensions of the interdigitated electrode were checked using LEXT OLS5100 confocal microscope (Olympus) and Merlin SEM (ZEISS) and processed with the manufacturer's software. Electrochemical impedance spectroscopy of the device, in contact with agarose pad, was performed using SP200 Potentiostat (BioLogic).

### Electrical stimulation of *S. epidermidis*

Electric stimulation was applied using an SP200 Potentiostat (BioLogic). One stimulation cycle consisted of 75 mVpp/μm, AC, 0.1 kHz for 10 s. For enhancing the inhibitory effect of antibiotics, *S. epidermidis* was preconditioned with five cycles of stimulation (1-min intervals) and then incubated with a sublethal concentration (30 μg/mL) of gentamicin for 18 h at 37°C. For drug-free biofilm suppression, stimulation cycles were applied periodically at 10-min intervals for 18 h at 37°C.

### Fluorescence microscopy

Short-term time-lapse images with an imaging duration under 10 min were acquired using a Stellaris 8 WLL confocal microscope (Leica Microsystems) with a 63× objective (63×/1.4 numerical aperture, UV transmission, oil immersion, 0.14 mm working distance, 506350). ThT fluorescence was detected with an excitation laser of 458 nm and an emission detection window of 490–545 nm using the HyD X2 detector. pHrodo fluorescence was detected with an excitation laser of 500 nm and an emission detection window of 530–600 nm using the HyD X2 detector. GTTR fluorescence was detected with an excitation laser of 595 nm and an emission detection window of 630–750 nm using the HyD S3 detector. For overnight time-lapse experiments, phase contrast images of *S. epidermidis* were captured using an Axio Observer 7 microscope (Zeiss) with a 100× or 63× objective (1.4 numerical aperture, oil immersion) in an incubator box maintained at 37°C. Images were background subtracted and adjusted for brightness and contrast using ImageJ.

### Intracellular pH assay with BCECF-AM

A total of 1 mL of the overnight cultured *S. epidermidis* was pelleted and resuspended in an equal volume of pH-adjusted TSB buffers. The resuspended bacterial solution was added to an aerated culture tube and incubated in a shaker incubator (37°C, 200 rpm) for 3 h. After the incubation, 25 μM BCECF-AM (Invitrogen) was added to the culture tubes and incubated at 30°C for 30 min. BCECF-AM fluorescence was measured using a Synergy NEO HTS Plate Reader according to the manufacturer's instructions. The Intracellular pH Calibration Buffer Kit (Invitrogen, P35379) was used to calibrate BCECF-AM fluorescence with intracellular pH, allowing for the quantification of transmembrane pH gradient ΔpH. Transmembrane proton gradient $\Delta H^+$ was measured by taking the negative anti-log of pH to find proton concentration $[H^+]$ to calculate $\Delta H^+ = [H^+]_{external} - [H^+]_{internal}$. For the kinetics experiment using BCECF-AM, fluorescence measurements were taken every minute in the Synergy NEO HTS Plate Reader. After 5 min, the plate was taken out and 150 μM CCCP or 3 μM nigericin (Invitrogen) was added to the wells. Upon addition, changes in BCECF-AM fluorescence were continuously monitored for 30 min.

### Measurement of ATP and growth

Upon applying the desired cycles of electrical stimulation, the agarose pad and electrode surface were flushed with TSB medium to collect *S. epidermidis*. Using a Synergy NEO HTS Plate Reader, the OD of the stimulated and non-stimulated cells was adjusted to $OD_{600}$ = 0.2. ATP levels in stimulated cells were measured using the BacTiter-Glo Microbial Cell Viability Assay and normalized to those of non-stimulated controls. For the measurement of growth, 200 μL of the $OD_{600}$ = 0.2 samples were added to a 96-well plate, and OD was monitored overnight using a Tecan Infinite 200 microplate reader at 37°C under orbital shaking. The percentage of biofilm formation was quantified using ImageJ by examining the area of coverage from phase contrast images taken after 18 h incubation.

### Electrical stimulation and characterization of porcine skin

Porcine skin (Fisher Scientific, NC1275387) was soaked in TSB buffer overnight before the experiment. *S. epidermidis*, 3 μL, was inoculated onto the porcine skin surface. pH 5-adjusted tragacanth gum (3% w/v, Sigma-Aldrich) was applied to the electrode surface (8 $\mu L/cm^2$). Finally, the electrode was placed on the inoculated porcine skin and BLAST treatment was applied, applying an electrical stimulation every 10 min for 18 h at 37°C. To quantify colony-forming units on the porcine skin, the skin and electrode were flushed with pH 7.4 TSB to collect the attached bacteria. The TSB containing the collected *S. epidermidis* was incubated for 6 h in an aerated bacterial culture tube before being inoculated on a TSB agar plate for colony counting. The identical procedure was used for BLAST treatment on silicone and polyethylene surfaces.

To determine the pH of porcine skin before and after applying tragacanth gum, a 1-$cm^2$ piece of skin was soaked in PBS at pH 7.4 overnight. After soaking, the skin was gently shaken to remove excess PBS, and MQuant pH-indicator strips (range: pH 5–10) were placed on the skin's surface. Then, 8 $\mu L/cm^2$ of pH 5 tragacanth gum was spread on the skin, and the pH was allowed to equilibrate for 10 min. Excess gum was gently dried off with a towel, and another pH-indicator strip was placed on the skin. The strip's color was analyzed by photographing it, converting the image to HSB stack in ImageJ, and quantifying the hue, saturation, and brightness. The quantified color was then compared to control strips applied to PBS and pH 5-tragacanth gum.

For SEM characterization, the porcine skin was fixed with 3% glutaraldehyde for 16 h at 4°C. The fixed porcine skin was subjected to increasing concentrations of acetone and isopropyl alcohol solvent series and dried with a Leica EM CPD300 Critical Point Drier following the manufacturer's protocol on preparing bacterial samples. The dried samples were sputtered with 8 nm of platinum/palladium using a Cressington Sputter Coater 208 and imaged with a Merlin FE SEM (Zeiss). The percentage of skin coverage was quantified using ImageJ by examining the area of coverage from the SEM images.

### Finite element simulations

Finite element analysis of the electric field distribution was conducted using COMSOL Multiphysics software. More details on the simulations can be found in Note S1.

### Real-time RT-qPCR

Details on the PCR, including the primer sequences, can be found in Note S2.

### Statistical analysis

OriginPro 2024 was employed for all statistical analyses. Unless stated otherwise, the error bars represent 1 SD. For biological data analysis, multiple t tests were performed. A significance threshold of $p < 0.05$ was used to determine statistical significance. In the figure panels, the following symbols were used to indicate significance levels: n.s., non-significant ($p > 0.05$); *$p < 0.05$; **$p < 0.01$; ***$p < 0.001$; ****$p < 0.0001$.

## RESOURCE AVAILABILITY

### Lead contact

Further information and requests for resources and reagents should be directed to and will be fulfilled by the lead contact, Bozhi Tian (btian@uchicago.edu).

### Materials availability

This study did not generate new unique materials.

### Data and code availability

- The data of this study are available within the article and supplemental information.
- The data reported in this paper will be shared by the lead contact upon request.
- This paper does not report original code.

## ACKNOWLEDGMENTS

B.T. and G.M.S. both acknowledge support from the Bill & Melinda Gates Foundation (INV-067331). B.T. acknowledges support from the US Army Research Office (W911NF-24-1-0053) and the National Science Foundation (DMR-2414222). G.M.S. acknowledges support from the National Institutes of Health (R35GM13964) and the US Army Research Office (W911NF-22-1-0107, W911NF-1-0361). We thank the staff at the Integrated Light Microscopy Core and Biophysics Core at the University of Chicago for their help.

## AUTHOR CONTRIBUTIONS

B.T. and G.M.S. supervised the research. S.K. designed and performed the research. S.K. discovered the concept of selective excitability and coined the term. S.K. fabricated all the devices. C.Y. assisted with a part of the device preparation. S.K., E.E., M.L., and A.Y. conducted the data analysis. A.Y., C.J.C., and E.E. assisted with the time-lapse experiment. S.K. and J.Y. performed the transcriptional analysis. J.S. assisted with a part of the schematics preparation. A.K. performed the COMSOL simulations. S.K., B.T., and G.M.S. prepared the manuscript, with input from all other authors.

## DECLARATION OF INTERESTS

The University of Chicago and the University of California, San Diego filed provisional patent applications for the electrical stimulation devices. S.K., B.T., and G.M.S. are the inventors.

## SUPPLEMENTAL INFORMATION

Supplemental information can be found online at https://doi.org/10.1016/j.device.2024.100596.

Received: August 8, 2024
Revised: September 13, 2024
Accepted: September 20, 2024
Published: October 24, 2024

## REFERENCES

1. Li, P., Kim, S., and Tian, B. (2024). Beyond 25 years of biomedical Innovation in nano-bioelectronics. Device *2*, 100401. https://doi.org/10.1016/j.device.2024.100401.
2. Li, P., Zhang, J., Hayashi, H., Yue, J., Li, W., Yang, C., Sun, C., Shi, J., Huberman-Shlaes, J., Hibino, N., and Tian, B. (2024). Monolithic silicon for high spatiotemporal translational photostimulation. Nature *626*, 990–998. https://doi.org/10.1038/s41586-024-07016-9.
3. Prominski, A., Shi, J., Li, P., Yue, J., Lin, Y., Park, J., Tian, B., and Rotenberg, M.Y. (2022). Porosity-based heterojunctions enable leadless optoelectronic modulation of tissues. Nat. Mater. *21*, 647–655. https://doi.org/10.1038/s41563-022-01249-7.
4. Nirenberg, S., and Pandarinath, C. (2012). Retinal prosthetic strategy with the capacity to restore normal vision. Proc. Natl. Acad. Sci. USA *109*, 15012–15017. https://doi.org/10.1073/pnas.1207035109.
5. Majmudar, A., Kim, S., Li, P., and Tian, B. (2024). Perspectives on non-genetic optoelectronic modulation biointerfaces for advancing healthcare. Med-X *2*, 18. https://doi.org/10.1007/s44258-024-00030-6.
6. Guyot, M., Simon, T., Ceppo, F., Panzolini, C., Guyon, A., Lavergne, J., Murris, E., Daoudlarian, D., Brusini, R., Zarif, H., et al. (2019). Pancreatic nerve electrostimulation inhibits recent-onset autoimmune diabetes. Nat. Biotechnol. *37*, 1446–1451. https://doi.org/10.1038/s41587-019-0295-8.
7. Balasubramanian, S., Weston, D.A., Levin, M., and Davidian, D.C.C. (2024). Charging Ahead: Examining the Future Therapeutic Potential of Electroceuticals. Adv. Ther. *7*, 2300344. https://doi.org/10.1002/adtp.202300344.
8. Balasubramanian, S., Weston, D.A., Levin, M., and Davidian, D.C.C. (2024). Electroceuticals: emerging applications beyond the nervous system and excitable tissues. Trends Pharmacol. Sci. *45*, 391–394. https://doi.org/10.1016/j.tips.2024.03.001.
9. Prindle, A., Liu, J., Asally, M., Ly, S., Garcia-Ojalvo, J., and Süel, G.M. (2015). Ion channels enable electrical communication in bacterial communities. Nature *527*, 59–63. https://doi.org/10.1038/nature15709.
10. Chen, Y.E., Fischbach, M.A., and Belkaid, Y. (2018). Skin microbiota-host interactions. Nature *553*, 427–436. https://doi.org/10.1038/nature25177.
11. Shi, J., Kim, S., Li, P., Dong, F., Yang, C., Nam, B., Han, C., Eig, E., Shi, L.L., Niu, S., et al. (2024). Active biointegrated living electronics for managing inflammation. Science *384*, 1023–1030. https://doi.org/10.1126/science.adl1102.
12. Severn, M.M., and Horswill, A.R. (2023). Staphylococcus epidermidis and its dual lifestyle in skin health and infection. Nat. Rev. Microbiol. *21*, 97–111. https://doi.org/10.1038/s41579-022-00780-3.
13. Otto, M. (2009). Staphylococcus epidermidis - The "accidental" pathogen. Nat. Rev. Microbiol. *7*, 555–567. https://doi.org/10.1038/nrmicro2182.
14. Dong, Y., Speer, C.P., and Glaser, K. (2018). Beyond sepsis: Staphylococcus epidermidis is an underestimated but significant contributor to neonatal morbidity. Virulence *9*, 621–633. https://doi.org/10.1080/21505594.2017.1419117.
15. Landemaine, L., Da Costa, G., Fissier, E., Francis, C., Morand, S., Verbeke, J., Michel, M.L., Briandet, R., Sokol, H., Gueniche, A., et al. (2023). Staphylococcus epidermidis isolates from atopic or healthy skin have opposite effect on skin cells: potential implication of the AHR pathway modulation. Front. Immunol. *14*, 1–19. https://doi.org/10.3389/fimmu.2023.1098160.
16. Hon, K.L., Tsang, Y.C.K., Pong, N.H., Leung, T.F., and Ip, M. (2016). Exploring Staphylococcus epidermidis in atopic eczema: friend or foe? Clin. Exp. Dermatol. *41*, 659–663. https://doi.org/10.1111/ced.12866.
17. Clavaud, C., Jourdain, R., Bar-Hen, A., Tichit, M., Bouchier, C., Pouradier, F., El Rawadi, C., Guillot, J., Ménard-Szczebara, F., Breton, L., et al. (2013). Dandruff Is Associated with Disequilibrium in the Proportion of the Major Bacterial and Fungal Populations Colonizing the Scalp. PLoS One *8*, e58203. https://doi.org/10.1371/journal.pone.0058203.
18. Cunha, B.A. (2001). antibiotic side effects. Med. Clin. North Am. *85*, 149–185. https://doi.org/10.1016/s0025-7125(05)70309-6.

19. Weidinger, S., Beck, L.A., Bieber, T., Kabashima, K., and Irvine, A.D. (2018). Atopic dermatitis. Nat. Rev. Dis. Primers *4*, 1. https://doi.org/10.1038/s41572-018-0001-z.

20. Larsson, D.G.J., and Flach, C.F. (2022). Antibiotic resistance in the environment. Nat. Rev. Microbiol. *20*, 257–269. https://doi.org/10.1038/s41579-021-00649-x.

21. Darby, E.M., Trampari, E., Siasat, P., Gaya, M.S., Alav, I., Webber, M.A., and Blair, J.M.A. (2023). Molecular mechanisms of antibiotic resistance revisited. Nat. Rev. Microbiol. *21*, 280–295. https://doi.org/10.1038/s41579-022-00820-y.

22. Lee, J.Y.H., Monk, I.R., Gonçalves da Silva, A., Seemann, T., Chua, K.Y.L., Kearns, A., Hill, R., Woodford, N., Bartels, M.D., Strommenger, B., et al. (2018). Global spread of three multidrug-resistant lineages of Staphylococcus epidermidis. Nat. Microbiol. *3*, 1175–1185. https://doi.org/10.1038/s41564-018-0230-7.

23. Koo, J., MacEwan, M.R., Kang, S.K., Won, S.M., Stephen, M., Gamble, P., Xie, Z., Yan, Y., Chen, Y.Y., Shin, J., et al. (2018). Wireless bioresorbable electronic system enables sustained nonpharmacological neuroregenerative therapy. Nat. Med. *24*, 1830–1836. https://doi.org/10.1038/s41591-018-0196-2.

24. Pavlov, V.A., and Tracey, K.J. (2022). Bioelectronic medicine: Preclinical insights and clinical advances. Neuron *110*, 3627–3644. https://doi.org/10.1016/j.neuron.2022.09.003.

25. Moritz, C., Field-Fote, E.C., Tefertiller, C., van Nes, I., Trumbower, R., Kalsi-Ryan, S., Purcell, M., Janssen, T.W.J., Krassioukov, A., Morse, L.R., et al. (2024). Non-invasive spinal cord electrical stimulation for arm and hand function in chronic tetraplegia: a safety and efficacy trial. Nat. Med. *30*, 1276–1283. https://doi.org/10.1038/s41591-024-02940-9.

26. Sultana, S.T., Babauta, J.T., and Beyenal, H. (2015). Electrochemical biofilm control: A review. Biofouling *31*, 745–758. https://doi.org/10.1080/08927014.2015.1105222.

27. Czerwińska-Główka, D., and Krukiewicz, K. (2020). A journey in the complex interactions between electrochemistry and bacteriology: From electroactivity to electromodulation of bacterial biofilms. Bioelectrochemistry *131*, 107401. https://doi.org/10.1016/j.bioelechem.2019.107401.

28. Kim, S., Eig, E., and Tian, B. (2024). The convergence of bioelectronics and engineered living materials. Cell Rep. Phys. Sci. *5*, 102149. https://doi.org/10.1016/j.xcrp.2024.102149.

29. Li, P., Kim, S., and Tian, B. (2022). Nanoenabled Trainable Systems: From Biointerfaces to Biomimetics. ACS Nano *16*, 19651–19664. https://doi.org/10.1021/acsnano.2c08042.

30. Benarroch, J.M., and Asally, M. (2020). The Microbiologist's Guide to Membrane Potential Dynamics. Trends Microbiol. *28*, 304–314. https://doi.org/10.1016/j.tim.2019.12.008.

31. Jones, J.M., and Larkin, J.W. (2021). Toward Bacterial Bioelectric Signal Transduction. Bioelectricity *3*, 116–119. https://doi.org/10.1089/bioe.2021.0013.

32. Stratford, J.P., Edwards, C.L.A., Ghanshyam, M.J., Malyshev, D., Delise, M.A., Hayashi, Y., and Asally, M. (2019). Electrically induced bacterial membrane-potential dynamics correspond to cellular proliferation capacity. Proc. Natl. Acad. Sci. USA *116*, 9552–9557. https://doi.org/10.1073/pnas.1901788116.

33. Sender, R., Fuchs, S., and Milo, R. (2016). Are We Really Vastly Outnumbered? Revisiting the Ratio of Bacterial to Host Cells in Humans. Cell *164*, 337–340. https://doi.org/10.1016/j.cell.2016.01.013.

34. Larkin, J.W., Zhai, X., Kikuchi, K., Redford, S.E., Prindle, A., Liu, J., Greenfield, S., Walczak, A.M., Garcia-Ojalvo, J., Mugler, A., and Süel, G.M. (2018). Signal Percolation within a Bacterial Community. Cell Syst. *7*, 137–145.e3. https://doi.org/10.1016/j.cels.2018.06.005.

35. Yang, C.Y., Bialecka-Fornal, M., Weatherwax, C., Larkin, J.W., Prindle, A., Liu, J., Garcia-Ojalvo, J., and Süel, G.M. (2020). Encoding Membrane-Potential-Based Memory within a Microbial Community. Cell Syst. *10*, 417–423.e3. https://doi.org/10.1016/j.cels.2020.04.002.

36. Comerci, C.J., Gillman, A.L., Galera-Laporta, L., Gutierrez, E., Groisman, A., Larkin, J.W., Garcia-Ojalvo, J., and Süel, G.M. (2022). Localized electrical stimulation triggers cell-type-specific proliferation in biofilms. Cell Syst. *13*, 488–498.e4. https://doi.org/10.1016/j.cels.2022.04.001.

37. Fang, Y., Prominski, A., Rotenberg, M.Y., Meng, L., Acarón Ledesma, H., Lv, Y., Yue, J., Schaumann, E., Jeong, J., Yamamoto, N., et al. (2021). Micelle-enabled self-assembly of porous and monolithic carbon membranes for bioelectronic interfaces. Nat. Nanotechnol. *16*, 206–213. https://doi.org/10.1038/s41565-020-00805-z.

38. Ortega, M.A., Fernández-Garibay, X., Castaño, A.G., De Chiara, F., Hernández-Albors, A., Balaguer-Trias, J., and Ramón-Azcón, J. (2019). Muscle-on-a-chip with an on-site multiplexed biosensing system for: In situ monitoring of secreted IL-6 and TNF-$\alpha$. Lab Chip *19*, 2568–2580. https://doi.org/10.1039/c9lc00285e.

39. Liu, N., and Gao, Y. (2017). Recent Progress in Micro-Supercapacitors with In-Plane Interdigital Electrode Architecture. Small *13*, 1–10. https://doi.org/10.1002/smll.201701989.

40. Chiera, S., Bosco, F., Mollea, C., Piscitello, A., Sethi, R., Nollo, G., Caola, I., and Tessarolo, F. (2023). Staphylococcus epidermidis is a safer surrogate of Staphylococcus aureus in testing bacterial filtration efficiency of face masks. Sci. Rep. *13*, 21807–21810. https://doi.org/10.1038/s41598-023-49005-4.

41. Lambers, H., Piessens, S., Bloem, A., Pronk, H., and Finkel, P. (2006). Natural skin surface pH is on average below 5, which is beneficial for its resident flora. Int. J. Cosmet. Sci. *28*, 359–370. https://doi.org/10.1111/j.1467-2494.2006.00344.x.

42. O'Goshi, K., Okada, M., Iguchi, M., and Tagami, H. (2002). The predilection sites for chronic atopic dermatitis do not show any special functional uniqueness of the stratum corneum: Measurements of the water barrier function, hydration state, skin surface lipids, corneocyte size and pH in patients and normal indi. Exog. Dermatol. *1*, 195–202. https://doi.org/10.1159/000066233.

43. Prakash, C., Bhargava, P., Tiwari, S., Majumdar, B., and Bhargava, R.K. (2017). Skin Surface pH in Acne Vulgaris: Insights from an Observational Study and Review of the Literature. J. Clin. Aesthet. Dermatol. *10*, 33–39.

44. Sim, P., Strudwick, X.L., Song, Y., Cowin, A.J., and Garg, S. (2022). Influence of Acidic pH on Wound Healing In Vivo: A Novel Perspective for Wound Treatment. Int. J. Mol. Sci. *23*, 13655. https://doi.org/10.3390/ijms232113655.

45. Proksch, E. (2018). pH in nature, humans and skin. J. Dermatol. *45*, 1044–1052. https://doi.org/10.1111/1346-8138.14489.

46. Lukić, M., Pantelić, I., and Savić, S.D. (2021). Towards optimal pH of the skin and topical formulations: From the current state of the art to tailored products. Cosmetics *8*, 69. https://doi.org/10.3390/cosmetics8030069.

47. Wang, T., Chen, H., Yu, C., and Xie, X. (2019). Rapid determination of the electroporation threshold for bacteria inactivation using a lab-on-a-chip platform. Environ. Int. *132*, 105040. https://doi.org/10.1016/j.envint.2019.105040.

48. Dorr, D. (2009). Determining Voltage Levels of Concern for Human and Animal Response to AC Current. In 2009 IEEE Power & Energy Society General Meeting (IEEE), pp. 1–6. https://doi.org/10.1109/PES.2009.5275848.

49. Krulwich, T.A., Sachs, G., and Padan, E. (2011). Molecular aspects of bacterial pH sensing and homeostasis. Nat. Rev. Microbiol. *9*, 330–343. https://doi.org/10.1038/nrmicro2549.

50. Padan, E., Zilberstein, D., and Schuldiner, S. (1981). pH homesstasis in bacteria. Biochim. Biophys. Acta *650*, 151–166. https://doi.org/10.1016/0304-4157(81)90004-6.

51. Chong, C.E., Bengtsson, R.J., and Horsburgh, M.J. (2022). Comparative genomics of Staphylococcus capitis reveals species determinants. Front. Microbiol. *13*, 1005949. https://doi.org/10.3389/fmicb.2022.1005949.

52. Lawal, O.U., Barata, M., Fraqueza, M.J., Worning, P., Bartels, M.D., Goncalves, L., Paixão, P., Goncalves, E., Toscano, C., Empel, J., et al. (2021). Staphylococcus saprophyticus From Clinical and Environmental Origins

Have Distinct Biofilm Composition. Front. Microbiol. *12*, 663768–663813. https://doi.org/10.3389/fmicb.2021.663768.

53. Lagadic-Gossmann, D., Huc, L., and Lecureur, V. (2004). Alterations of intracellular pH homeostasis in apoptosis: Origins and roles. Cell Death Differ. *11*, 953–961. https://doi.org/10.1038/sj.cdd.4401466.
54. Lee, D.Y.D., Galera-Laporta, L., Bialecka-Fornal, M., Moon, E.C., Shen, Z., Briggs, S.P., Garcia-Ojalvo, J., and Süel, G.M. (2019). Magnesium Flux Modulates Ribosomes to Increase Bacterial Survival. Cell *177*, 352–360.e13. https://doi.org/10.1016/j.cell.2019.01.042.
55. Tormo, M.Á., Martí, M., Valle, J., Manna, A.C., Cheung, A.L., Lasa, I., and Penadés, J.R. (2005). SarA is an essential positive regulator of Staphylococcus epidermidis biofilm development. J. Bacteriol. *187*, 2348–2356. https://doi.org/10.1128/JB.187.7.2348-2356.2005.
56. Wang, C., Li, M., Dong, D., Wang, J., Ren, J., Otto, M., and Gao, Q. (2007). Role of ClpP in biofilm formation and virulence of Staphylococcus epidermidis. Microbes Infect. *9*, 1376–1383. https://doi.org/10.1016/j.micinf.2007.06.012.
57. Fey, P.D., and Olson, M.E. (2010). Current concepts in biofilm formation of Staphylococcus epidermidis. Future Microbiol. *5*, 917–933. https://doi.org/10.2217/fmb.10.56.
58. Williams, M.R., Bagood, M.D., Enroth, T.J., Bunch, Z.L., Jiang, N., Liu, E., Almoughrabie, S., Khalil, S., Li, F., Brinton, S., et al. (2023). Staphylococcus epidermidis activates keratinocyte cytokine expression and promotes skin inflammation through the production of phenol-soluble modulins. Cell Rep. *42*, 113024. https://doi.org/10.1016/j.celrep.2023.113024.
59. Gawande, P.V., Leung, K.P., and Madhyastha, S. (2014). Antibiofilm and antimicrobial efficacy of Dispersinb®-KSL-w peptide-based wound gel against chronic wound infection associated bacteria. Curr. Microbiol. *68*, 635–641. https://doi.org/10.1007/s00284-014-0519-6.
60. Brackman, G., De Meyer, L., Nelis, H.J., and Coenye, T. (2013). Biofilm inhibitory and eradicating activity of wound care products against staphylococcus aureus and staphylococcus epidermidis biofilms in an in vitro chronic wound model. J. Appl. Microbiol. *114*, 1833–1842. https://doi.org/10.1111/jam.12191.
61. Schierle, C.F., De La Garza, M., Mustoe, T.A., and Galiano, R.D. (2009). Staphylococcal biofilms impair wound healing by delaying reepithelialization in a murine cutaneous wound model. Wound Repair Regen. *17*, 354–359. https://doi.org/10.1111/j.1524-475X.2009.00489.x.
62. Taghavizadeh Yazdi, M.E., Nazarnezhad, S., Mousavi, S.H., Sadegh Amiri, M., Darroudi, M., Baino, F., and Kargozar, S. (2021). Gum tragacanth (Gt): A versatile biocompatible material beyond borders. Molecules *26*, 1510. https://doi.org/10.3390/molecules26061510.
63. Uhm, C., Jeong, H., Lee, S.H., Hwang, J.S., Lim, K.M., and Nam, K.T. (2023). Comparison of structural characteristics and molecular markers of rabbit skin, pig skin, and reconstructed human epidermis for an ex vivo human skin model. Toxicol. Res. *39*, 477–484. https://doi.org/10.1007/s43188-023-00185-1.
64. Michels, M., and Bakker, E.P. (1985). Generation of a large, protonophore-sensitive proton motive force and pH difference in the acidophilic bacteria Thermoplasma acidophilum and Bacillus acidocaldarius. J. Bacteriol. *161*, 231–237. https://doi.org/10.1128/jb.161.1.231-237.1985.
65. Mulkidjanian, A.Y., Dibrov, P., and Galperin, M.Y. (2008). The past and present of sodium energetics: May the sodium-motive force be with you. Biochim. Biophys. Acta *1777*, 985–992. https://doi.org/10.1016/j.bbabio.2008.04.028.
66. Pirbadian, S., Chavez, M.S., and El-Naggar, M.Y. (2020). Spatiotemporal mapping of bacterial membrane potential responses to extracellular electron transfer. Proc. Natl. Acad. Sci. USA *117*, 20171–20179. https://doi.org/10.1073/PNAS.2000802117.
67. Liu, X., Gao, H., Ward, J.E., Liu, X., Yin, B., Fu, T., Chen, J., Lovley, D.R., and Yao, J. (2020). Power generation from ambient humidity using protein nanowires. Nature *578*, 550–554. https://doi.org/10.1038/s41586-020-2010-9.
68. Shi, J., Lin, Y., Li, P., Mickel, P., Sun, C., Parekh, K., Ma, J., Kim, S., Ashwood, B., Meng, L., et al. (2024). Monolithic-to-focal evolving biointerfaces in tissue regeneration and bioelectronics. Nat. Chem. Eng. *1*, 73–86. https://doi.org/10.1038/s44286-023-00008-y.
69. Li, Z., Misra, R.P., Li, Y., Yao, Y.C., Zhao, S., Zhang, Y., Chen, Y., Blankschtein, D., and Noy, A. (2023). Breakdown of the Nernst–Einstein relation in carbon nanotube porins. Nat. Nanotechnol. *18*, 177–183. https://doi.org/10.1038/s41565-022-01276-0.
70. Tang, T.C., An, B., Huang, Y., Vasikaran, S., Wang, Y., Jiang, X., Lu, T.K., and Zhong, C. (2020). Materials design by synthetic biology. Nat. Rev. Mater. *6*, 332–350. https://doi.org/10.1038/s41578-020-00265-w.
71. Long, Y., Wei, H., Li, J., Yao, G., Yu, B., Ni, D., Gibson, A.L., Lan, X., Jiang, Y., Cai, W., and Wang, X. (2018). Effective Wound Healing Enabled by Discrete Alternative Electric Fields from Wearable Nanogenerators. ACS Nano *12*, 12533–12540. https://doi.org/10.1021/acsnano.8b07038.
72. Huang, Y., Yao, K., Zhang, Q., Huang, X., Chen, Z., Zhou, Y., and Yu, X. (2024). Bioelectronics for electrical stimulation: materials, devices and biomedical applications. Chem. Soc. Rev. *53*, 8632–8712. https://doi.org/10.1039/d4cs00413b.
73. Saw, T.B., Gao, X., Li, M., He, J., Le, A.P., Marsh, S., Lin, K.h., Ludwig, A., Prost, J., and Lim, C.T. (2022). Transepithelial potential difference governs epithelial homeostasis by electromechanics. Nat. Phys. *18*, 1122–1128. https://doi.org/10.1038/s41567-022-01657-1.
74. Dawson, T.W., Stuchly, M.A., and Kavet, R. (2004). Evaluation of interactions of electric fields due to electrostatic discharge with human tissue. IEEE Trans. Biomed. Eng. *51*, 2194–2198. https://doi.org/10.1109/TBME.2004.834293.